Jour. of the KGS, Vol. 20, No. 7. September 2004, pp. 57~68

Lateral Earth Pressure Caused by Action on Earth Retaining Wall in Clay Foundation Ground with Consideration of Construction Speed

지중 구조물에 작용하는 측방토압에 대한 성토 재하 속도의 영향

Im, Eun-Sang[1] 임 은 상
Lee, Kang-Il[2] 이 강 일

요 지

연약점토지반에 성토 등의 상재하중을 재하하게 되면 측방유동이라고 하는 측방변위가 발생하게 된다. 이 측방유동은 파일기초의 변형, 교대의 이동, 지중매설관의 파괴 등 성토에 인접한 지중구조물에 피해를 가하게 된다. 그렇지만, 측방유동은 체적변형과 전단변형도 동시에 발생할 뿐만 아니라 이 측방유동에 영향을 미치는 인자가 많기 때문에 측방유동에 의해서 발생하는 측방토압의 발생 메커니즘이 아직 명확히 밝혀지지 않았다. 그리고 최근 근접시공 등 기존구조물에 근접해서 공사가 진행되는 경우가 많아 이러한 근접구조물에 어떠한 피해를 가할 것인가 또는 대책공법을 설계하기 위한 설계하중으로서 측방토압을 구해야 하는 필요성이 커지고 있는 것 또한 현실이다. 그러므로 본 연구에서는 성토에 의해서 연약지반에 발생하는 측방토압에 미치는 재하속도의 영향을 조사하기 위해서 실내모형실험을 실시하였다. 그 결과, 측방토압이 삼각형 분포를 이룬다는 것과 재하속도가 빠를수록 측방토압의 최대치가 커지고 부등침하가 커진다는 것을 알 수 있었다. 그리고 이러한 재하속도의 영향은 부의 dilatancy에 의한 과잉간극수압의 발생에 기인한다는 것을 알았다.

Abstract

When an embankment is constructed on soft clay ground, the lateral displacement generally called as lateral flow is generated in the foundation ground. It strongly affects stabilities of structures, such as foundation piles and underground pipes, in and on the foundation ground. The lateral earth pressure induced by the lateral flow is influenced by the magnitude and construction speed of embankment, the geometric conditions and geotechnical characteristics of the embankment, and the foundation ground, and so on. Accurate methods for estimating the lateral earth pressure have not ever been established because the lateral flow of a foundation ground shows very complicated behavior, which is caused by the interaction of shear deformation and volumetric deformation. In this paper, a series of model tests were carried out in order to clarify effects of construction speed of an embankment on the lateral earth pressure in a foundation ground were design. It was found that the magnitude and the distribution of the lateral earth pressure and its change with time are dependent on the construction speed of the embankment. It was found that a mechanism for the lateral earth pressure was generated by excess pore water pressure due to negative dilatancy induced by shear deformation under the different conditions of construction speeds of embankments.

Keywords : Clay ground, Construction speed, Embankment, Lateral earth pressure, Theory of elasticity

1 Member, Post doctoral Researcher, Korea Institute Water and Environment, KOWACO (esim89@hanmail.net)
2 Member, Associate Prof. Dept. of Civil Engrg. Deajin Univ.

1. Introduction

Stresses in ground are changed and deformed when structures are constructed on the ground even if the ground does not fail. Therefore, when a new structure is constructed on the ground, it is necessary to consider the effects of the stress changes and deformations in the ground, which would probably affect structures that had been constructed in and on the ground. When an embankment is constructed on a soft clay ground, the ground does not only settle in the vertical direction but also deforms in the horizontal direction. The horizontal deformation is generally called as a lateral flow of ground. This lateral flow has become one of the most important issues in geotechnical studies in recent years. From these studies, it was found that 75% of the total surface settlement and 60% of the entire horizontal deformation occur during the period of an embankment construction (Ortiz 1967), and that the amount of horizontal deformation increases rapidly when the safety factor of the embankment against failure is less than a certain value, e.g. safety factor of 1.3 by Tavenas et al. (1978, 1980) 1.5 by Marche and Chapuis (1974), and Yamaguchi et al. (1981). The maximum horizontal deformation due to embankment load is generated at a depth of 1/3 of the layer thickness from the top of a soft clay layer (Shibata et al., 1982). A number of relationships between the maximum surface settlement and the maximum horizontal deformation were proposed by Akai et al. (1974), Yamaguchi et al. (1980), Tavenas et al. (1979, 1980), and others. Extensive numerical approaches on the estimation of horizontal deformation have also been carried out. For example, Poulos (1972) pointed out that the computed horizontal displacements do not agreed with those of measured and listed the possible reasons. Almeida et al. (1985) stated that pore water pressures and their dissipation rates were very well predicted, as were the maximum values of both horizontal and vertical displacements, but the displacement profiles with depth were not so. Sekiguchi et al. (1994) reported that the calculated horizontal displacements under the toe of an embankment using an elasto-viscoplastic model had generally good aggrement with the measured quantifies.

The lateral flow strongly affects a stabilities of structures in and on the foundation ground. Serious damages were often reported for foundation piles (Heyman and Boersma 1961; Leussink and Wenz 1969; Bigot et al. 1977), underground pipes, and bridge abutments (Stermac et al. 1968; Marche and Lacroix 1972). Infrastructure facilities close to an embankment suffere from unforeseen lateral earth pressure induced by the lateral flow of the foundation ground. This implies that the lateral earth pressure induced by the lateral flow of the foundation ground is a very important factor as an external force in evaluating the stabilities of underground structures.

So far numorous theoretical and experimental studies on effects of the lateral flow on the foundation piles have been carried out, e.g. Poulos and Davies (1980), Carter (1982), Broms et al. (1987), Springman (1989), and Stewart et al. (1992). Not only to mitigate damages of foundation piles but also in design of sheet piles and continuous walls constructed to reduce the deformation of the foundation ground, it is necessary to estimate the lateral earth pressure acting on those structures. For this reason, an appropriate method for estimating the lateral earth pressure induced by the lateral flow of a foundation ground should be developed. However, because the lateral flow of the foundation ground is caused by both volumetric deformation attributed to consolidation and the shear deformation, it is difficult to estimate the exact amount of lateral earth pressure.

The main factors affecting the lateral earth pressure can be listed as the magnitude of embankment load, construction method of embankment, geometric conditions and geotechnical characteristics of embankment and foundation ground. Therefore, a method for estimating the lateral earth pressure must consider these factors. Therefore, this paper focused on the effects of the construction speeds of embankment to the lateral earth pressure caused in the foundation ground.

Because the magnitude and distribution of the lateral earth pressure depend on the strength of foundation ground, a homogeneous ground with a uniformly

distributed strength was selected for 1G-model tests in this study and thereby loading to find the influence of the construction speed of embankment as the factor affecting the lateral earth pressure. In addition, centrifuge model tests are planned following a series of the 1G-model tests in this study. The magnitude and distribution of the lateral earth pressure are to be investigated in the centrifuge model tests on the foundation ground, where the strength increases with depth, in order to clarify the difference of the strength distribution in the foundation ground behavior.

The model tests were carried out herein to estimate the lateral earth pressures either on the sheet piles or continuous rigid walls that are installed to reduce the lateral flow at the toe of the embankment. It is well known that the magnitude of the lateral earth pressure is dependent on the rigidity of a retaining structure for the lateral flow. The magnitudes of the lateral earth pressures acting on high rigid structures, such as continuous concrete walls, are larger than those acting on flexible structures, such as sheet piles. In practice, the largest value in the predicted lateral earth pressure is often used as a design value in the viewpoint of safety. In this study, the lateral earth pressure acting on the rigid retaining structures installed at the toe of an embankment, which is considered to be the largest value, was investigated using a model container as shown in Fig. 1.

It was found from the test results that the magnitude and the distribution of the lateral earth pressure and their change with time are varied with the construction speed of an embankment. Observations of tests were compared with the results of numerical solutions for estimating stresses caused by an embankment load based on the elasticity theory.

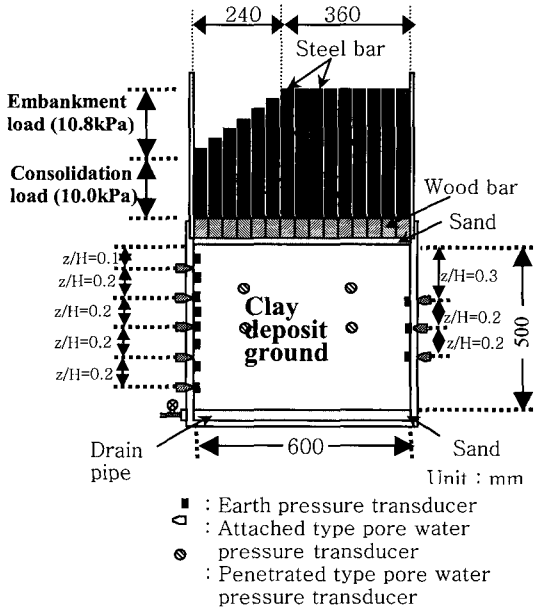

Fig. 1. Schematic of model ground with pore and earth pressure transducers

2. Laboratory Model Tests

2.1 Material Properties

The clay used was alluvial marine clay called Dejima clay, which obtained from Hiroshima Bay, Japan. The collected clay was remolded and sieved through 0.047 mm mesh and stored in plastic containers. The physical and mechanical properties of this clay are listed in Tables 1 and 2. The clay was remolded with water content about twice the liquid limit and the clay slurry was poured into a vacuum container. The slurry was mixed and de-aired in the vacuum container under a pressure of over 700 mmHg for 6 hours.

Table 1. Physical properties of Dejima clay

Specific Gravity, Gs	Liquid Limit, WL (%)	Plastic Limit, WP (%)	Plasticity Index, IP
2.651	86.0	40.0	46.0

Table 2. Mechanical properties of Dejima clay

Rate of strength increase, cu/p	Coefficient of consolidation at 10 kPa, Cv (cm^2/min)	Compression index, Cc	Swelling index, Cs	Pore pressure parameter at failure, A	Shear strength in Vane shear test, c_u (kPa)
0.43	0.22	0.739	0.063	0.74	2.65

2.2 Apparatus and Test Procedure

In this study, the lateral earth pressure acting on a rigid retaining structure installed at the toe of an embankment, which is considered to be the largest value, was investigated using a model container as shown in Fig. 1. The model container used was 600 mm in length and 200 mm in width. Its height was 850 mm during the preconsolidation and 500 mm during the embankment loading. The length of the model container was made as twice as long as the length of the embankment slope. The gradient of the embankment slope was set to be 1:0.45 whereas the unit weight of embankment material is 20 kN/m^3. Because the gradient of embankment slope in the case of neighboring constructions causing problems of the lateral flow is generally made large by reinforced earth methods or others, a large gradient of embankment slope was used in this study. The height of the model container was determined to have enough depth so as to obtain a peak value of the lateral earth pressure in the vertical distributions based on the elasticity theory and the FEM analyses derived in this study. To negate the effects of sidewall friction, the width of the model container was desired to have enough width and sidewalls of model container were lubricated with silica grease. In this study, however, 200 mm of the width was determined consi- dering the maximum value due to the limitation of the preparation of the volume of the clay slurry in the laboratory. The model container was made by acrylic plates. The steel plates were fixed around the model container to prevent the deformation of acrylic plates due to the action of the earth pressures. Eight pore water transducers of the attached type (PS-1KC, Max.=98 kPa, Kyowa Co.), four pore water transducers of the penetrated type (PDCR81, Max.=98 kPa, Druck Limited Co.) and eleven earth pressure transducers (PGM-1KG, Max.=98 kPa, Kyowa Co.) were installed in order to measure the excess pore water pressure and the lateral earth pressure at various locations as shown in Fig. 1.

The test procedure is as follows. First, the pore water pressure transducers of the attached type and the earth pressure transducers were set on the side of acrylic plates as shown in Fig. 1. Then, the de-aired slurry is poured into the model container up to the depth of about 800 mm. The clay deposit is consolidated under the self-weight of the slurry for about 5 days and under the preconsolidation pressure of 10 kPa applied through steel bars as shown in Fig. 1 for about 2 months. After the preconsolidation, the thickness of the model ground becomes about 500 mm and then four pore water pressure transducers of the penetrated type are installed in the clay ground. The preconsolidation pressure of 10 kPa is applied for 5 days to remove influence of stress release during the installation of the penetrated type pore water pressure transducers.

The drainage was permitted at the top and bottom of the model ground during consolidation stage. After the completion of the preconsolidation, the clay deposit is further loaded by steel bars shaping an embankment with a load intensity of 10.8 kPa under double drainage condition as shown in Fig. 1. The load intensity of 10.8 kPa is determined from the stability analysis which gives the safety factor of 1.26 by following equation.

$$Fs = \frac{q_u}{p} = \frac{5.14 c_u}{p} \quad (1)$$

Test cases were adopted to investigate the influence of construction speed and of geometric conditions of an embankment, which are defined by ratio of slope length a to crest length b, to the lateral earth pressure in the model clay ground as shown in Table 3.

When the loading rate was 1.54 kPa/min, Case 1 was carried out under single stage loading of 10.8kPa, while the rest of the cases were carried out under three stages loading of 3.1 kPa, 3.1 kPa and 4.6 kPa. Because the interval of each fill loading is decided upon the degree

Table 3. Patterns of test

Case	Loading, p (kPa)	Rate index, t^*	Shape index, b/a
Case 1	10.8	0.003	2.30
Case 2	10.8	0.067	2.30
Case 3	10.8	0.675	2.30
Case 4	10.8	2.0	2.30
Case 5	10.8	0.675	1.33

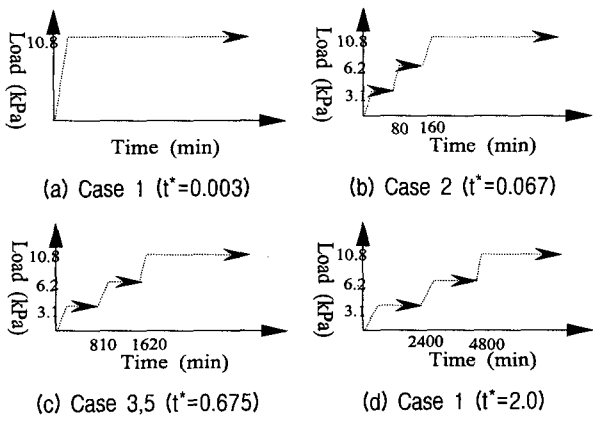

(a) Case 1 (t^*=0.003) (b) Case 2 (t^*=0.067)

(c) Case 3,5 (t^*=0.675) (d) Case 1 (t^*=2.0)

Fig. 2. Patterns of loading

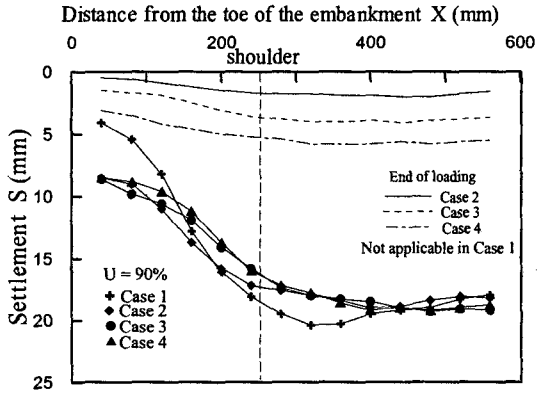

Fig. 3. Surface settlement of clay ground

of consolidation in the actual construction works, the loading of the second and third stages in Cases 2, 3, 4, and 5 were started as shown in Fig. 2 when the degree of consolidation of the previous loading stage reached U=30, 60, 90, and 60%, respectively. The rate indices t* can be calculated by Eq. (2), and Shape index b/a is a rate of slope and crest of embankment. The rate index t* is given as:

$$t^* = \frac{t_e}{\frac{T_{90} \cdot (H/2)^2}{c_v}} \qquad (2)$$

where t_e, T_{90}, and c_v are the construction duration of embankment, the time factor at the degree of consolidation of U=90% and the coefficient of consolidation, respectively.

3. Test Results and Discussion

3.1 Surface Settlement

Figure 3 shows the surface settlements of the foundation ground, which were measured by location of each steel bar during test, immediately after the loading and at the degree of consolidation of U=90% in all cases. The degree of consolidation, U, is defined by the amount of the surface settlement at a point 160 mm from the center of the embankment. The peak value of the surface settlement appeared at the position where the distance from the toe of the embankment was about X=300 mm and minimum one generated at the toe of the embankment, and it is found that the shear deformation occurs by this differential settlement. Moreover, comparing the surface settlements at the immediate end of loading and at the degree of consolidation of U=90%, the shear deformation is generated even in the consolidation stage and is still larger in Case 1 than the others. Therefore, it was found that the shear deformation is caused not only in the loading stage but also in the consolidation stage and it influences the lateral earth pressure and the excess pore water pressure.

3.2 Dissipation of Excess Pore Water Pressure

The variations of excess pore water pressures with time after the end of the final loading under the toe of embankment and under the center of embankment in Case 1 are presented in Figs. 4 (a) and (b), respectively. In these figures, the excess pore water pressures are normalized by the applied embankment load. From Fig. 4 (a), despite the equal distance to the drainage surface, there is a difference in the dissipation of the excess pore water pressures between at z/H=0.1 and at Z/H=0.9 after the start of consolidation. This is because the dissipation of the excess pore water pressure at the upper layer of the foundation ground was obstructed by a development of the excess pore water pressure caused by the dilatancy due to the shear deformation and its influence remained up to about 7000 min when the degree of consolidation U is approximately 85%. The same tendency was also seen at z/H=0.3 and 0.7. The difference of the excess

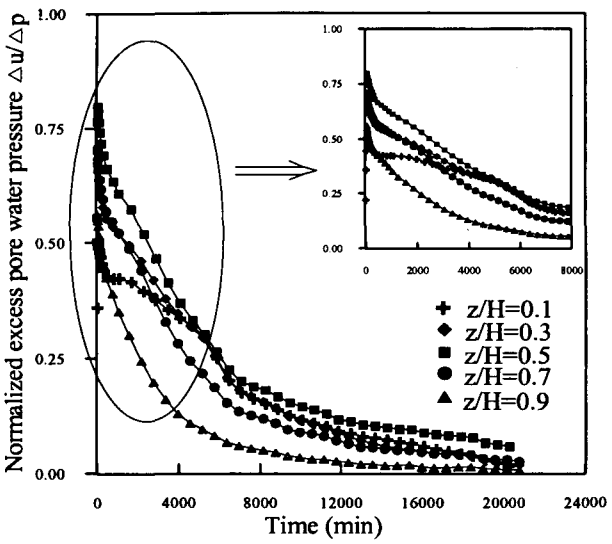

(a)under the toe of embankment

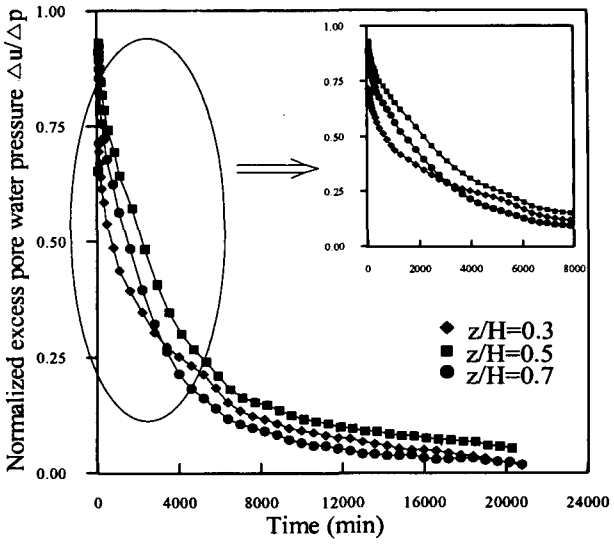

(b) under the center of embankment

Fig. 4. Excess pore water pressure under the toe of embankment in Case 1

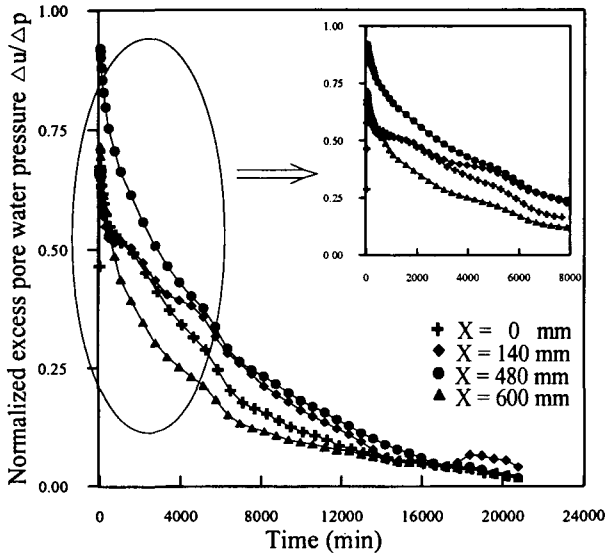

Fig. 5. Excess pore water pressure at z/H=0.3 in Case 1

pore water pressures between z/H=0.3 and z/H=0.7 is smaller than that between z/H=0.1 and z/H= 0.9. The shear deformation generated in the foundation ground is larger in the upper portion than in the lower portion. The same tendency also appeared in the other cases too. However, the dissipation of the excess pore water pressures is varied similarly with time under the center of embankment as shown in Fig. 4 (b).

Figure 5 shows the variations of excess pore water pressures with time after the end of the final loading at different distances from the toe of embankment to X=0 mm, 140 mm, 480 mm and 600 mm in the same depth of z/H=0.3 in Case 1. Despite the same depth, the different dissipation behavior of the excess pore water pressure is observed in the early consolidation stage. The dissipation of the excess pore water pressure is slower under the slope of embankment than under the center of embankment. This difference is considered to be caused by the shear deformation, which generates largely under the slope of the embankment than in the other part by an unbalance of the applied vertical load.

The isochrones of the excess pore water pressure under the toe of embankment in Cases 1 and 3 are shown in Figs. 6 (a) and (b), respectively. In these figures, the excess pore water pressures are normalized by the applied embankment load. The elapsed time was started to be counted at the end of the final loading. From Fig. 6, it is clear that the shape of the measured isochrones of the excess pore water pressure is different from a shape of ordinary isochrones that have the same value at the same distance from the drainage surface. This is considered to be caused by the following reasons. The first is that the excess pore water pressures in the upper layer of foundation ground are slowly dissipated due to the development of the excess pore water pressure induced by the shear deformation in the loading and the consolidation stages. Unfortunately, there was no method

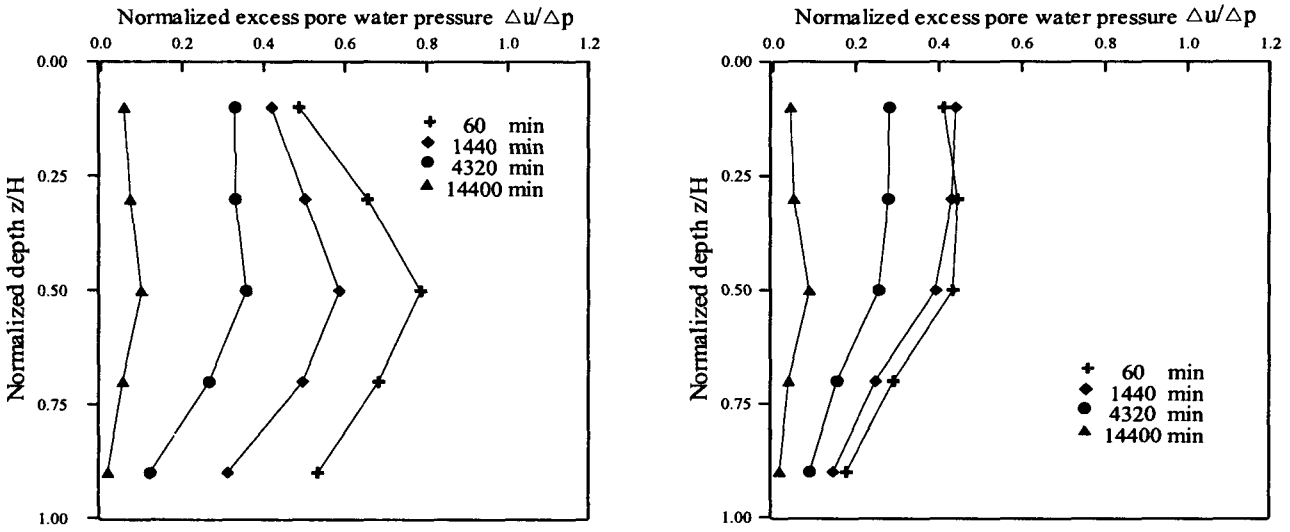

Fig. 6. Isochrons of the excess pore water pressure under the toe of embankment

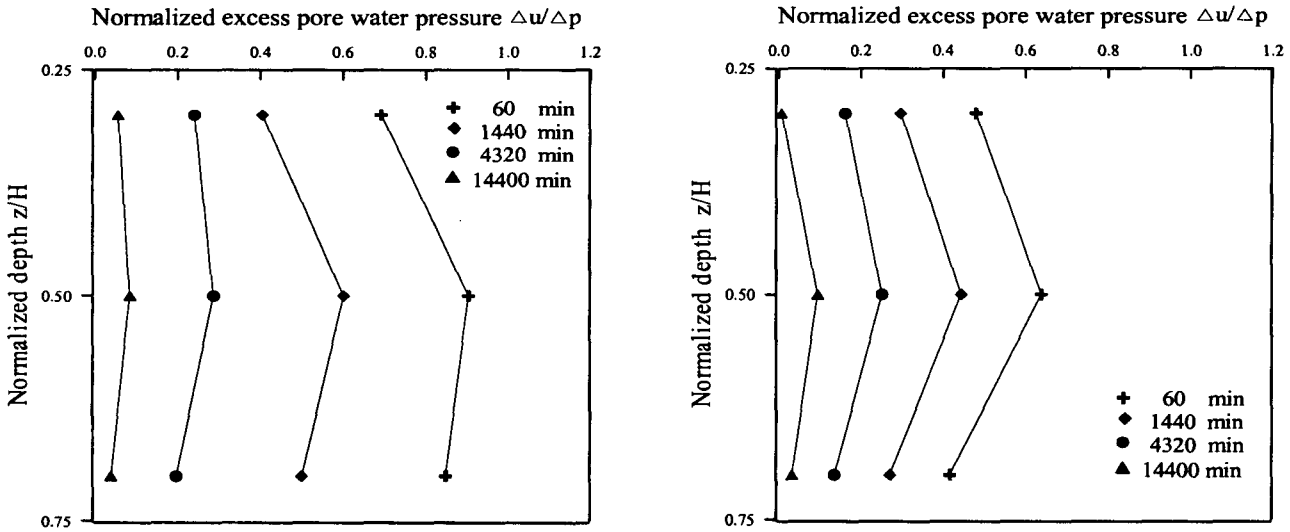

Fig. 7. Isochrons of the excess pore water pressure under the center of embankment

to directly measure the amount of the shear deformation, which is considered to be generated largely in the upper layer of the foundation ground. The second is that the sand layer laid on the foundation ground did not act as a perfect drainage boundary because of the existence of the wood bar closely resting on the upper sand layer.

The isochrones of the excess pore water pressure under the center of embankment at the same time as Fig. 7 after the end of the final loading in Cases 1 and 3 are shown in Figs. 7 (a) and (b), respectively. They found to be different from those under the toe of embankment and are symmetric with respect of the middle depth of z/H=0.5. Because of these evidences, the first reason mentioned above is considered to be a stronger factor for the phenomenon that the dissipation of the excess pore water pressure under the toe of embankment was slower in the upper layer than in the lower layer.

3.3 Variation of Lateral Earth Pressure with Time and Depth

The variation of the lateral earth pressures with time after the end of the final loading under the toe of embankment in Case 3 is shown in Fig. 8. The large

lateral earth pressures are generated in the loading stage and the early consolidation stage, and thereafter decrease with time in the consolidation stage. Specifically, the lateral earth pressure at z/H=0.3 rapidly decreased with time. On the other hand, the lateral earth pressure at z/H=0.78 is relatively smaller than that at the upper layer in the loading stage and hardly decreases with time in the consolidation stage. This difference of the lateral earth pressure between the upper layer and lower layer is considered to be due to the undrained shear deformation caused in the upper layer of the foundation ground in the loading stage as mentioned previously. Figs. 9 and 10 show the variation of the lateral earth pressures with time after the end of the final loading at z/H=0.3 and 0.4 under the toe of the embankment, respectively. The lateral earth pressures at z/H=0.3 in all cases were largely generated in the loading stage and in the early consolidation stage, and rapidly decrease in the consolidation stage as mentioned above. On the other hand, the generated lateral earth pressures at z/H=0.4 in all cases gradually decrease in the consolidation stage in comparison with those at z/H=0.3, and particularly the lateral earth pressures re-increase at 3000-4000min because the lateral earth pressure due to progressive slide is larger than dissipation of the excess pore water pressure induced by the shear deformation. In comparison with the effect of the construction speed of embankment, the lateral earth pressures generated in the loading stage are slightly increase with the increase of construction speed of embankment but the lateral earth pressures in the consolidation stage are reduced to the same value except at z/H=0.3 in Case 1 despite the difference of the construction speed of embankment. This phenomenon is considered to be due to the reason that the shear deformation which resulted from the differential settlement causing the lateral earth pressure increases with an increase of the construction speed of embankment.

Vertical distributions of the lateral earth pressures with depth under the toe of embankment in Cases 1 and 3 are shown in Figs. 11 (a) and (b), respectively. In these figures, the lateral earth pressure and the depth are normalized by the applied embankment load and the

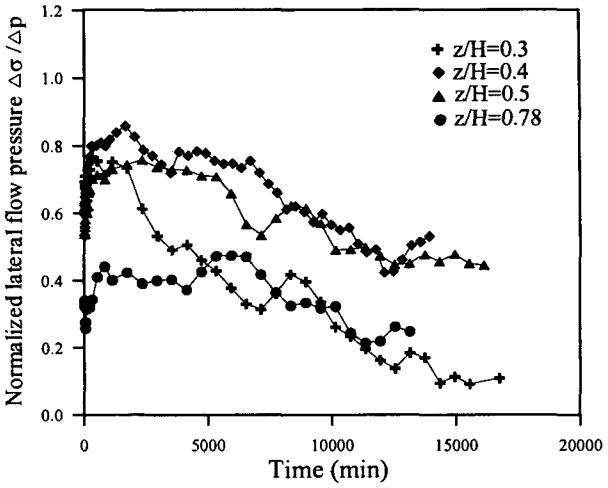

Fig. 8. Lateral earth pressure with time in Case 3

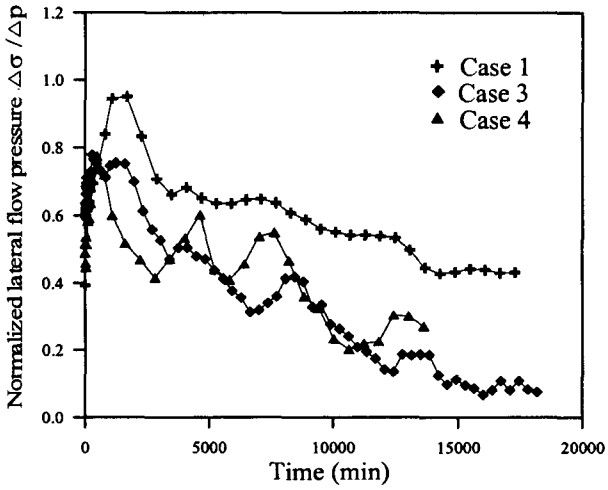

Fig. 9. Lateral earth pressure with time at z/H=0.3

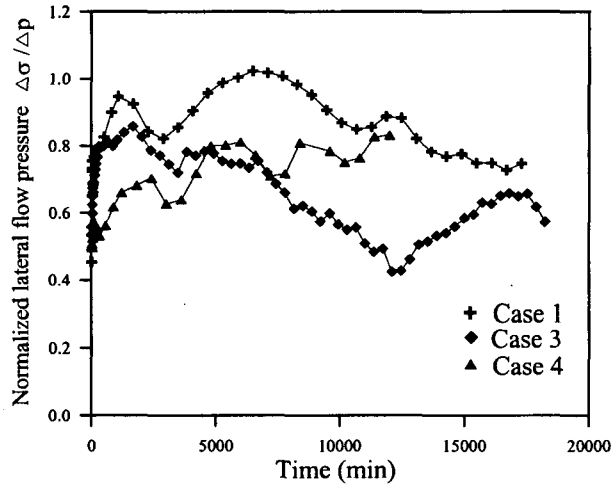

Fig. 10. Lateral earth pressure with time at z/H=0.4

thickness of the foundation ground, respectively. The time elapsed was started to be counted at the end of the final loading. The vertical distributions of the lateral

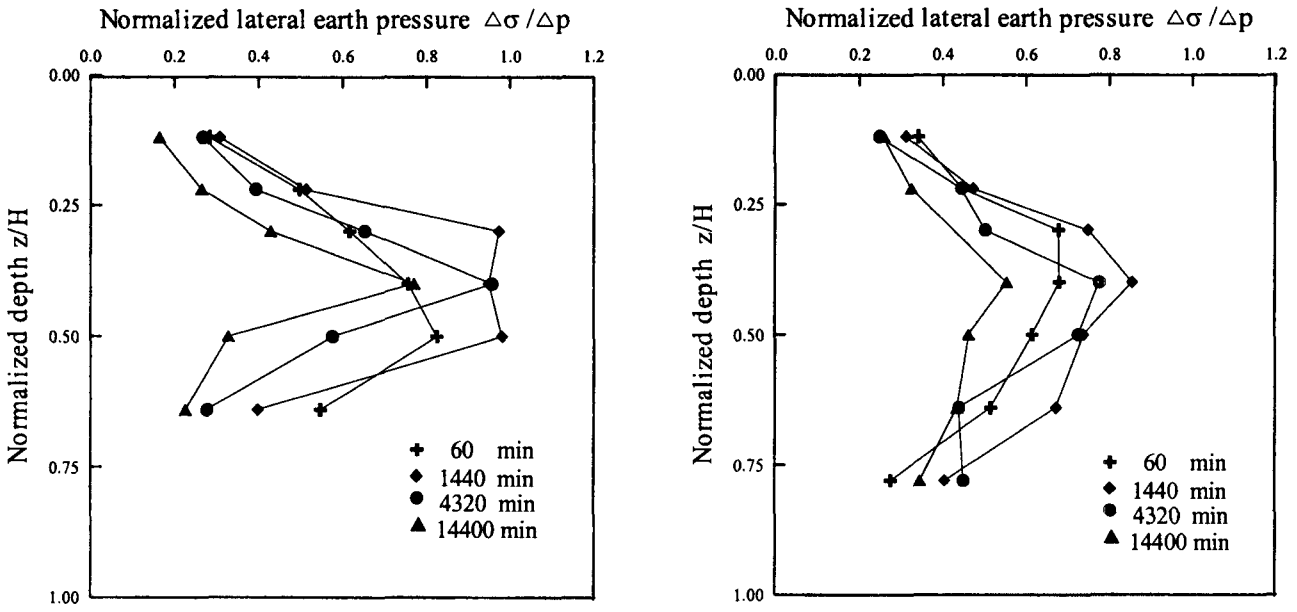

Fig. 11. Vertical distributions of lateral earth pressure

earth pressures can be regarded as a triangular distribution and the maximum values of the lateral earth pressure ($\Delta\sigma_h/\Delta P$) are 0.8～1.0. Moreover, it is seen that the maximum lateral earth pressure is influenced by the construction speed of embankment.

The detailed discussion on the maximum lateral earth pressure, which increases with an increase in the construction speed of embankment, will be given in Section 3.4. In Case 1 shown in Fig. 11 (a), the peak point of the triangular distribution was at z/H=0.5 in the early stage of consolidation and then moved to z/H=0.4 in the later stage of consolidation. However, in Case 3 shown in Fig. 11 (b), the peak point of the triangular distribution was at z/H=0.3 in the early stage of consolidation and then moved to z/H= 0.4 in the later stage of consolidation. In the evaluation of the earth pressures acting on the side of the retaining structures, it should be noted that the peak point of the earth pressure is moving upward in Case 1 and downward in Case 3. The movement of peak point of the measured lateral earth pressure in Case 1 is considered because the all embankment load is constructed before the excess pore water pressure of each load step is hardly dissipated. However, The movement of that in Case 3 is considered to be due to the generation of pressures by the shear deformation at upper part of model ground in comparison with the middle part because the shear deformation is generated during loading stage.

3.4 Effect of Construction Speed of Embankment

Figure 12 presents the effect of the construction speed of embankment on the maximum excess pore water pressure in the vertical distribution which was normalized

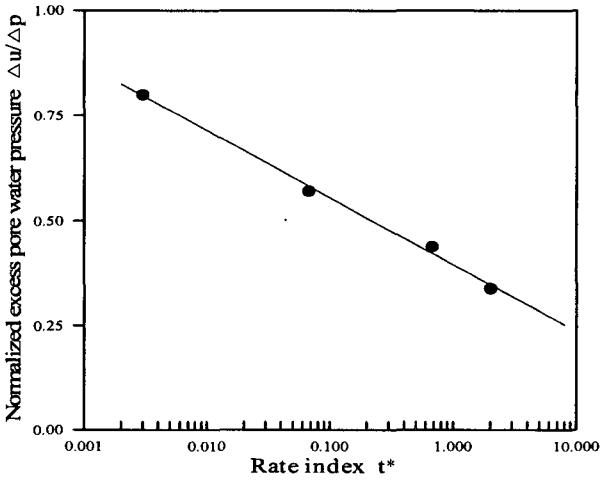

Fig. 12. Effect of construction speed of embankment on excess pore water pressure normalized by embankment load

by the applied embankment load. In this figure, the construction speed of embankment is expressed by the rate index t* defined by Eq. (2). The relationship of decrease of maximum excess pore water pressure with the increase of the construction speed of the embankment is shown in this figure. Moreover, the maximum excess pore pressure did not reach to the applied embankment load even in Case 1. The maximum excess pore water pressures did not appear in the immediate end of loading and were generated on the way in the consolidation stage.

The effects of the construction speed of embankment on the maximum lateral earth pressures in the vertical distribution in all test durations and at the end of the tests are also shown in Fig. 13. In this figure, the lateral earth pressures were normalized by the applied embankment load. The lateral earth pressures at the end of the tests were found to occur at the effective stress state because the excess pore water pressures have almost dissipated. It is clear that the maximum lateral earth pressure in the vertical distribution through all test duration decreases with the increase of the construction speed of embankment. The similar tendency is also seen in the results at the end of the tests.

The normalized depth where the maximum lateral earth pressure occured was a constant value of about 0.5 in spite of the difference of the construction speed of embankment as shown in Fig. 14. In this figure, It is found from this figure that the normalized depth where the maximum lateral earth pressure appeared constant and was not influenced by the geometric conditions of embankment.

Figure 15 presents the lateral earth pressure which is subtract the excess pore water pressure induced by dilatancy from the maximum lateral earth pressure in order to verify the effect of the excess pore water pressure induced by dilatancy. In this figure, the construction speed of embankment is expressed by the rate index t*. From Fig. 15, relationship between the normalized maximum lateral earth pressure and the rate index is more rapid than that of the maximum excess pore water pressures at z/H=0.3 and 0.5. If the excess pore water pressure induced by dilatancy was deducted

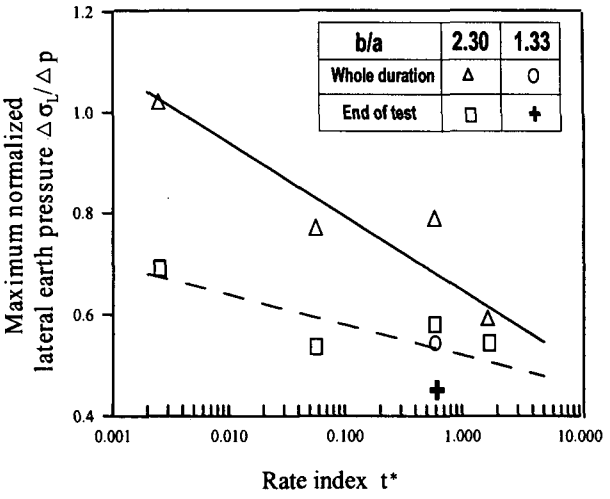

Fig. 13. Effect of construction speed of embankment on lateral earth pressure normalized by embankment load

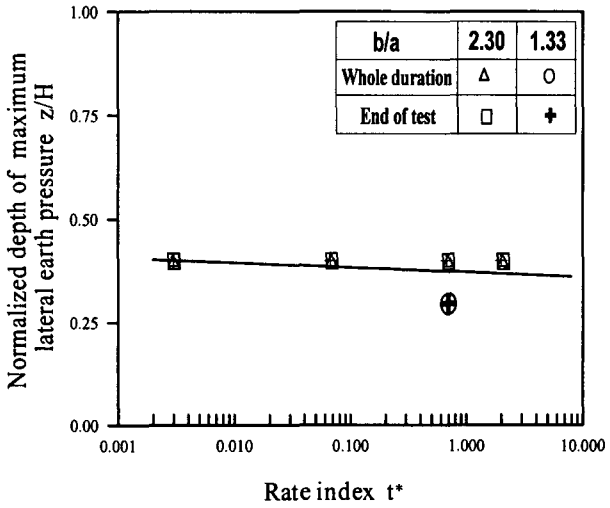

Fig. 14. Effect of construction speed of embankment on depth of the maximum lateral earth pressure

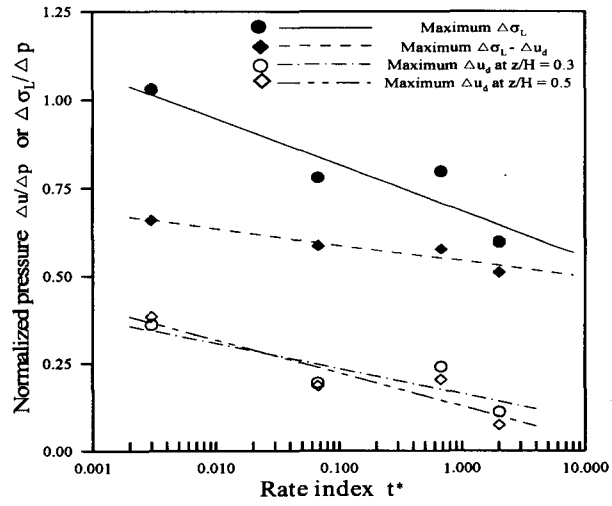

Fig. 15. Effect of construction speed of embankment on excess pore water pressure induced by dilatancy

from the maximum lateral earth pressure, it could be seen that an inclination of the relationship between the deducted maximum lateral earth pressure and the rate index becomes much slight. Therefore, it can be concluded here that once the increased excess pore water pressure induced by dilatancy is dissipated from the positions, where the shear deformation is easier to occur under the embankment, then the effect of the construction speed of embankment would diminish considerably.

4. Conclusions

The following conclusions can be made from the results of the model tests.

(1) When the construction speed of embankment increased, the amount of the surface settlements at the center and the toe of embankment decreased though at slightly inside of the embankment shoulder increased. The position of the peak value of the surface settlement was changed from the center of embankment to slightly inside of the embankment shoulder and the shear deformation under the slope of the embankment in clay ground increased with the increase of the construction speed of the embankment.

(2) The excess pore water pressure at the upper clay layer under the toe of embankment was larger and its dissipation was slower than that at the lower clay layer. This is considered to be due to the shear deformation, which occurred largely in the upper clay layer than in the lower clay layer in the loading stage and the early consolidation stage. The maximum excess pore water pressure occurring at the middle of the clay layer under the toe of embankment increased with the increase of the construction speed of embankment and a unique relationship between the maximum excess pore water pressure and the construction speed of embankment was recognized.

(3) The vertical distribution of the lateral earth pressure can be regarded as a triangular distribution. The maximum value of the lateral earth pressure was about 0.6～1.0 times the magnitude of the applied embankment load. The maximum value of the lateral earth pressure increased with increase of the construction speed of an embankment and was generated after some lapse of time after the end of loading. The depth where the maximum value of the lateral earth pressure appeared did not vary with the change of the construction speed of the embankment.

Acknowledgements

The authors wish to thank Mr. H. Yamamoto for his assistance with the design and construction of the apparatus. Mr. H. Kinoshita and Ms. Y. Shintaku are also acknowledged for their aid in completing this study.

References

1. Akai, K., Shibata, T., Tominaga, M., and Tamura, T. (1974), "Analysis of lateral displacement to be caused by embankment loading in ore-yard", *The 21st Proc. JSSMFE*, pp.1275-1278.
2. Almeida, M. S. S., Britto, A. M., and Parry, R. H. G. (1985), "Numerical modelling of a centrifuged embankment on soft clay", *Canadian Geotechnical Journal*, Vol.23, pp.103-114.
3. Bigot, G., Bourges, F., Frank, R., and Guegan, Y. (1977), "Action du deplacement lateral du sol sur un pieu", *The 9th Int. Conf. Soil Mech. And Foun. Eng.*, Tokyo, Japan, Vol.I, pp.407-401.
4. Broms B.B., Pandey, P.C., and Goh, A.T.C. (1987), "The lateral displacement of piles from embankment loads", *Proc. Japan SocCiv. Eng.*, 338/III-8 (12), pp.1-11.
5. Carter, J.P. (1982), "A numerical method for pile deformations due to nearby surface loads", *The 4th Int. Conf. Numer. Methods in Geotech.*, Ottawa, Canada, Vol.2, pp.811-817.
6. Heyman, L. and Boersma, L. (1961), "Bending moments in piles due to lateral earth pressure", *The 5th Int. Conf. Soil Mech. And Foun. Eng.*, Paris, France, Vol.II, pp.425-429.
7. Im, E. S. & Moriwaki, T. (2001), "Effect of the construction speed of embankment on settlement and lateral flow pressure in soft clay ground", *Symposium of JSSMFE*, Japanese Geotechnical Society, pp.109-114.
8. Im, E. S., Moriwaki, T. and Shintaku, Y. (2001), "Effect of the construction speed of embankment on lateral flow pressure in soft clay ground", *36th Conf. of JSSMFE*, pp.1447-1448.
9. Im, E. S., Moriwaki, T. and Shintaku, Y. (2002), "A simple method for predicting lateral flow pressure in clay ground under embankment", *Tsuchi-to-Kiso*, Japanese Geotechnical Society, Vol.50, No.2, pp.19-21.
10. Marche, R. and Chapuis, R. (1974), "Controle de la stabilite des remblais par mesure des deplacements horizontaux", *Canadian Geotechnical Journal*, Vol.1, pp.182-201.
11. Marche, R. and Lacroix, Y. (1972), "Stabilite des culees de ponts

etablies sur des pieux traversant une couche molle", *Canadian Geotechnical Journal*, pp.1-24.
12. Ortiz, I.S. (1967), "Zumpango test embankment", *Proc. ASCE*, Vol.93, No.SM-4, pp.199-209.
13. Poulos, H. G. (1972), "Difficulties in prediction of horizontal deformations of foundations", *Journal of the Soil Mechanics and Foundation Division*, ASCE, pp.843-848.
14. Poulos, H. G. and Davis, E.H. (1980): "*Pile foundation analysis design*", John Wiley & Sons, Inc.
15. Sekiguchi, H., Rowe, R.K., Ogawa, T., and Lo, K.Y. (1994), "Predicted behaviour of a test embankment using elasto-viscoplastic constitutive model", *The 29th Proc. JSSMFE*, pp. 1327-1330.
16. Shibata, T., Nomura, K., and Sekiguchi, H. (1982), "The behaviour of soft foundation under embankment", *The 17th Proc. JSSMFE*, pp.2017-2020.
17. Springman, S.M. (1989), "Lateral loading of piles due to simulated embankment construction", PhD thesis, Univ. of Cambridge, England.
18. Stewart, D.P. (1992), "Lateral loading of piled bridge abutment due to embankment construction", PhD thesis, Univ. of Western Australia, Australia.
19. Stermac, A.G., Devata, M. and Selby, K.G. (1968), "Unusual movements of abutments supported on end bearing piles", *Canadian Geotechnical Journal*, Vol.5, pp.69-79.
20. Tavenas, F., Blanchet, R., Garneau, R., and Leroueil, S. (1978), "The stability of stage-constructed embankments on soft clay", *Canadian Geotechnical Journal*, Vol.15, pp.283-305.
21. Tavenas, F., Mieussens, C. and Bourges, F. (1979), "Lateral displacements in clay foundations under embankments", *Canadian Geotechnical Journal*, Vol.16, pp.532-550.
22. Tavenas, F. and Leroueil, S. (1980), "The behaviour of embankments on clay foundations", *Canadian Geotechnical Journal*, Vol.17, pp.236-26.
23. Yamaguchi, H., Nakanodo, H., and Kitazume, M. (1980), "Model loading test of soft clay ground", *The 15th Proc. JSSMFE*, pp.853-856.
24. Yamaguchi, H., Nakanodo, H., and Kitazume, M. (1981), "Consolidation -deformation behavior of normal consolidation clay ground in the model test", *The 16th Proc. JSSMFE*, pp.817-820.

(received on Apr. 1, 2004, accepted on Aug. 10, 2004)